Dinuclear Oxomolybdate(V) Species with Oxalato and Pyridine Ligands Revisited: *cis*/*trans* Isomerization of $[Mo_2O_4(\eta^2\text{-}C_2O_4)_2(R\text{-}Py)_2]^{2-}$ (R-Py = Pyridine, Alkyl-Substituted Pyridine) in Water Evidenced by NMR Spectroscopy

Barbara Modec,*[a] Darko Dolenc,[a] Jurij V. Brenčič,[a] Jože Koller,[a] and Jon Zubieta[b]

Keywords: Isomerization / Molybdenum / N ligands / NMR spectroscopy / Polyoxometalates

The simple oxohalomolybdate(V) ions $[MoOCl_4(H_2O)]^-$ and $[MoOBr_4]^-$ were reacted with oxalic acid in mixtures containing an alcohol and a pyridine (R-Py) to form the dinuclear anions $[Mo_2O_4(\eta^2\text{-}C_2O_4)_2(R\text{-}Py)_2]^{2-}$ based on the $\{Mo_2O_4\}^{2+}$ structural core. The dinuclear anion exists in two isomeric forms – as a *trans* and as a *cis* isomer. A *trans* arrangement of the pyridine ligands relative to the $Mo_2(\mu_2\text{-}O)_2$ bridge was observed for $(PyH)_2[Mo_2O_4(\eta^2\text{-}C_2O_4)_2Py_2]$ (**1**), $(PyH)_2[Mo_2O_4(\eta^2\text{-}C_2O_4)_2(3,5\text{-}Lut)_2]$ (**2**), $[MeNC_5H_3(Me)_2]_2[Mo_2O_4(\eta^2\text{-}C_2O_4)_2(3,5\text{-}Lut)_2]\cdot H_2O$ (**3**), $(4\text{-}MePyH)_2[Mo_2O_4(\eta^2\text{-}C_2O_4)_2(4\text{-}MePy)_2]\cdot 1/2(4\text{-}MePy)$ (**5**), and $[(C_6H_5)_4P]_2[Mo_2O_4(\eta^2\text{-}C_2O_4)_2Py_2]\cdot H_2O$ (**7**) [Py = pyridine; 3,5-Lut = 3,5-lutidine; $MeNC_5H_3(Me)_2^+$ = *N*-methyl-3,5-lutidinium cation and 4-MePy = 4-methylpyridine], while a *cis* arrangement was found in only two compounds, namely $(4\text{-}EtPyH)_2[Mo_2O_4(\eta^2\text{-}C_2O_4)_2(4\text{-}EtPy)_2]$ (**4**) (4-EtPy = 4-ethylpyridine) and $(4\text{-}MePyH)_3[Mo_2O_4(\eta^2\text{-}C_2O_4)_2(4\text{-}MePy)_2]Br$ (**6**). The solution chemistry of the *trans*-$[Mo_2O_4(\eta^2\text{-}C_2O_4)_2Py_2]^{2-}$ anion was monitored by ^1H and ^{13}C variable temperature NMR spectroscopy and showed evidence of two processes: the substitution of a pyridine ligand for water, coupled with *cis*/*trans* isomerization. Both reactions were exploited in the preparation of *trans*-$(PyH)_2[Mo_2O_4(\eta^2\text{-}C_2O_4)_2(H_2O)_2]$ (**8**) from a water/methanol solution of *cis*-$(4\text{-}EtPyH)_2[Mo_2O_4(\eta^2\text{-}C_2O_4)_2(4\text{-}EtPy)_2]$ (**4**). *trans*-$(PyH)_2[Mo_2O_4(\eta^2\text{-}C_2O_4)_2(H_2O)_2]$ (**8**) was seen to react with methanol with the rupture of the molybdenum-to-oxalate bonds resulting in the cyclic octanuclear anion which crystallizes as a pyridinium salt, $(PyH)_2[Mo_8O_{16}(OCH_3)_8(\mu_8\text{-}C_2O_4)]\cdot 2CH_3OH$ (**9**). The compounds were fully characterized by X-ray structural analysis and IR spectroscopy. MO calculations were performed on the isomeric pair of $[Mo_2O_4(\eta^2\text{-}C_2O_4)_2(4\text{-}MePy)_2]^{2-}$ in order to establish their relative energies.

Introduction

The MoO^{3+} structural unit pervades in the chemistry of molybdenum in the +5 oxidation state.[1] The metal displays a marked tendency to dimerize through one or two oxygen bridges with the formation of the $\{Mo_2O_3\}^{4+}$ and $\{Mo_2O_4\}^{2+}$ dinuclear fragments. In the case of the $\{Mo_2O_4\}^{2+}$ structural core a direct interaction between two molybdenum atoms, conveniently described as a single metal–metal bond, is formed. The X-ray structural analyses of numerous $\{Mo_2O_4\}^{2+}$ compounds have shown that the basic structural properties of the $\{Mo_2O_4\}^{2+}$ core are independent of the ligands which complete the five- or sixfold coordination environments of the metal.[1,2] In the absence of ligands, the metal centers attain coordinative saturation through further assembly of $\{Mo_2O_4\}^{2+}$ units which share their originally μ_2-bridging oxo groups to form discrete oligonuclear clusters.[3] For instance, the association of four $\{Mo_2O_4\}^{2+}$ units through the agency of methoxide ions has been shown to produce two different types of octanuclear metal oxide cores: (i) a ring-like $\{Mo_8O_8(\mu_2\text{-}O)_8(\mu_2\text{-}OCH_3)_8\}$,[4,5] and (ii) a more compact $\{Mo_8O_8(\mu_3\text{-}O)_4(\mu_2\text{-}O)_4(\mu_3\text{-}OCH_3)_2(\mu_2\text{-}OCH_3)_4\}^{2+}$ core.[6] In the presence of suitable ligands, their ligation to the $\{Mo_2O_4\}^{2+}$ core normally precedes the self-assembly of dinuclear subunits. Multidentate oxygen donor ligands, in particular oxalate, with its well-known ability to adopt different coordination modes, can theoretically connect the dinuclear $\{Mo_2O_4\}^{2+}$ units into polymeric materials. True polymeric $\{Mo_2O_4\}^{2+}$ species where multidentate oxygen donor ligands link the dinuclear building blocks into infinite structures are extremely rare. The only examples are $[Mo_2O_4(C_2O_4)Cl_2]_n^{2n-}$ and $[Mo_2O_4(C_2O_4)_2(H_2PO_4)]_n^{3n-}$, with infinite chain structures, and $[Mo_2O_4(PO_4)(HPO_4)]_n^{3n-}$, with an infinite layer structure.[7–9] The bridging ligand in $[Mo_2O_4(C_2O_4)Cl_2]_n^{2n-}$ is oxalate, while in the other two polymers the phosphate

[a] Department of Chemistry and Chemical Technology, University of Ljubljana, Aškerčeva 5, 1000 Ljubljana, Slovenia.
Fax: +386-1-2419-220
E-mail: barbara.modec@guest.arnes.si
[b] Department of Chemistry, Syracuse University, Syracuse, New York 13244, USA
E-mail: jazubiet@syr.edu
Supporting information for this article is available on the WWW under http://www.eurjic.org or from the author.

  DOI: 10.1002/ejic.200500023

serves to link the dinuclear subunits. The literature also reports on another type of polymeric compound where the repeating structural unit is a tetranuclear, cube-like metal oxide core with the formula $\{Mo_4O_4(\mu_3\text{-}O)_4\}^{4+}$ and the bridging ligands are the phosphates.[10] The cube-like core may be considered as the assembly of two $\{Mo_2O_4\}^{2+}$ units. Apparently, under the reaction conditions employed, the assembly of $\{Mo_2O_4\}^{2+}$ units took place first and was followed by phosphate coordination to the periphery of the $\{Mo_4O_4(\mu_3\text{-}O)_4\}^{4+}$ core.

We have demonstrated in our previous work that a series of complexes with the oxalate bonded in different ways can be obtained by tuning the oxalate-to-molybdenum ratio: $[Mo_8O_{16}(OCH_3)_8(\mu_8\text{-}C_2O_4)]^{2-}$ and $[Mo_2O_4(\mu_2\text{-}C_2O_4)Cl_2]_n^{2n-}$ when the oxalate amounts were small, and *trans*-$[Mo_2O_4(\eta^2\text{-}C_2O_4)Py_2]^{2-}$ and $[\{Mo_2O_4(\eta^2\text{-}C_2O_4)_2\}_2(\mu_4\text{-}C_2O_4)]^{6-}$ when the amounts of the ligand were large.[7,11] Furthermore, with an even larger amount of the oxalate, $\{Mo_2O_4\}^{2+}$ no longer formed, but rather the $\{Mo_2O_3\}^{4+}$ core with four coordination sites per metal center. The species obtained, $[Mo_2O_3(\eta^2\text{-}C_2O_4)_4]^{4-}$, thus contains two oxalato ligands per molybdenum. Although the X-ray structure analyses provided unambiguous characterization of the above-listed complexes, their solubility in water and their diamagnetic nature enabled NMR solution studies. The spectrum of the pyridine-coordinated complex *trans*-$[Mo_2O_4(\eta^2\text{-}C_2O_4)Py_2]^{2-}$ displays broadening of the pyridine resonances, which suggested substitution reactions in water solutions. Further studies were therefore initiated with the aim to provide an adequate explanation of these observations.

Results and Discussion

Structural Studies

Structures of Compounds with trans- and cis-$[Mo_2O_4(\eta^2\text{-}C_2O_4)_2(R\text{-}Py)_2]^{2-}$ Anions

The *trans* and *cis* geometric isomers of the $[Mo_2O_4(\eta^2\text{-}C_2O_4)_2(R\text{-}Py)_2]^{2-}$ ion are depicted in Figures 1 and 2, respectively. A central $\{Mo_2O_4\}^{2+}$ core, with a pyridine ligand and a bidentate oxalate completing the six-coordinate environment of each metal, may be recognized in both isomers. The position of the pair of pyridine ligands or oxalates can be either on the opposite sides of the plane defined by the Mo=O groups (*trans* isomer) or on the same side (*cis* isomer). The *trans* arrangement was observed for R-Py = pyridine (**1** and **7**), 3,5-lutidine (**2** and **3**), and 4-methylpyridine (**5**), while *cis* isomers were found for 4-ethylpyridine (**4**) and 4-methylpyridine (**6**). Both isomers were isolated only in the case of 4-methylpyridine. The two isomeric forms of the dinuclear anion differ in symmetry: neglecting the alkyl substituents on the pyridine rings, the *trans* isomer belongs to the C_2 point group, and the *cis* isomer to the C_s point group. However, the above-stated symmetry of the anions is rarely realized in solid-state structures. The exceptions are the *trans* anions in **1** and **2**, where the center of the $Mo(\mu_2\text{-}O)_2Mo$ group sits on a crystallographic twofold rotation axis and only half of the anion defines the asymmetric unit. The geometric parameters of the $\{Mo_2O_4\}^{2+}$ core in compounds **1**–**7** do not differ significantly and have similar values to those determined previously for many other $\{Mo_2O_4\}^{2+}$ compounds:[1,2] (i) a short Mo–Mo distance in the range 2.5430(3)–2.5559(5) Å for *trans* isomers and 2.5519(2)–2.5520(3) Å for *cis* isomers, signifying a single metal–metal bond, and (ii) a nonplanar $Mo(\mu_2\text{-}O)_2Mo$ moiety with fold angles in the ranges 149.5(2)–154.07(9)° and 152.17(5)–153.88(6)° for *trans* and *cis* isomers, respectively. The *trans* influence of the terminal oxo group is reflected in the nonequivalence of the two molybdenum-to-oxalate oxygen bond lengths. Relevant geometric parameters for the anions in **1**–**7** are summarized in Tables 1 and 2.

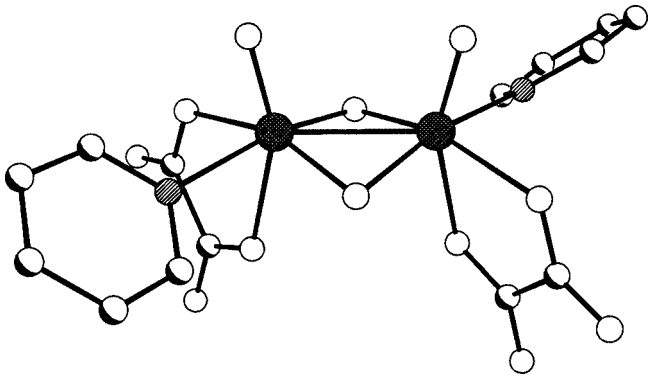

Figure 1. Ball-and-stick representation of the *trans*-$[Mo_2O_4(\eta^2\text{-}C_2O_4)_2(Py)_2]^{2-}$ anion in **1**. Mo sites are cross-hatched, nitrogen atoms are lined bottom left to top right, and oxygen atoms are small, unshaded and carbon atoms small, shaded spheres. The same drawing scheme is used throughout.

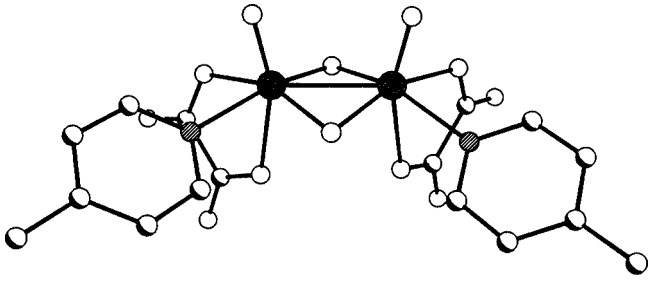

Figure 2. Ball-and-stick representation of the *cis*-$[Mo_2O_4(\eta^2\text{-}C_2O_4)_2(4\text{-}MePy)_2]^{2-}$ anion in **6**.

Interesting patterns of hydrogen bonds are observed for compounds **1**–**7**. The oxalato ligands, which can act as acceptors of hydrogen bonds, are matched with protonated pyridine molecules, and these are seen to form either a hydrogen bonding interaction with one noncoordinated oxygen atom from the oxalate or a bifurcated interaction with both noncoordinated oxygen atoms of the oxalate (Figure 3). The former type is present in **1**, with relatively short N···O distances of 2.642(2) Å, while the latter occurs in **2** and **5**. In the case of bifurcated hydrogen bonds, one is shorter than the other, as illustrated by **2**, where the N···O distances are 2.700(2) and 2.984(2) Å. Another type of hy-

Table 1. Selected geometric parameters [Å, °] for *trans*-$[Mo_2O_4(\eta^2\text{-}C_2O_4)_2(R\text{-}Py)_2]^{2-}$.

Compound	Mo–O(oxalate)	Mo–Mo	Fold angle[a]	Mo–N
1	2.135(1) vs. 2.189(1)	2.5490(3)	149.56(4)	2.257(2)
2	2.132(1) vs. 2.185(1)	2.5525(3)	151.58(4)	2.266(2)
3	2.129(2) vs. 2.167(1)	2.5488(2)	149.87(4)	2.246(2)
				2.257(2)
	2.127(2) vs. 2.180(2)			
5[b]	2.135(3) vs. 2.195(3)	2.5559(5)	150.2(2)	2.246(3)
				2.260(3)
	2.140(3) vs. 2.198(3)			
	2.130(3) vs. 2.200(3)	2.5492(5)	149.5(2)	2.247(4)
				2.253(4)
	2.142(3) vs. 2.184(3)			
7	2.118(2) vs. 2.176(2)	2.5430(3)	154.07(9)	2.268(2)
				2.310(2)
	2.127(2) vs. 2.155(2)			

[a] Defined as the dihedral angle between two $Mo(\mu_2\text{-}O)_2$ planes. [b] Two sets of parameters are listed, one for each anion in the asymmetric unit.

Table 2. Selected geometric parameters [Å, °] for *cis*-$[Mo_2O_4(\eta^2\text{-}C_2O_4)_2(R\text{-}Py)_2]^{2-}$.

Compound	Mo–O(oxalate)	Mo–Mo	Fold angle	Mo–N
4	2.115(1) vs. 2.212(1)	2.5520(3)	153.88(6)	2.241(2)
				2.260(2)
	2.086(1) vs. 2.185(1)			
6	2.117(1) vs. 2.229(1)	2.5519(2)	152.17(5)	2.233(1)
				2.251(1)
	2.113(1) vs. 2.207(1)			

drogen-bonding interaction is observed for the *cis* isomers: the position of the protonated aromatic ring is such as to form two interactions to two closest coordinated oxygen atoms of two different oxalates (Figure 3). As exemplified by **4**, one of the two N···O distances is shorter than the other [2.728(2) vs. 2.977(2) Å]. In **3** and **7**, with no cations able to participate in hydrogen-bonding interactions, hydrogen bonds occur between the oxalato ligands and the water molecules of crystallization instead. For instance, in **3** each water molecule forms two hydrogen bonds to two noncoordinated oxalate oxygens from two different anions, with O···O distances of 2.904(3) and 2.986(3) Å. Infinite chains of alternating dinuclear anions and water molecules are thus formed (Figure 3). In **3** the chains propagate along the *b* axis.

Structure of trans-(PyH)$_2$[Mo$_2$O$_4$(η^2-C$_2$O$_4$)$_2$(H$_2$O)$_2$] (8)

The structure of **8** consists of dinuclear *trans*-$[Mo_2O_4(\eta^2\text{-}C_2O_4)_2(H_2O)_2]^{2-}$ anions (shown in Figure 4) and protonated pyridine molecules as countercations. The asymmetric unit

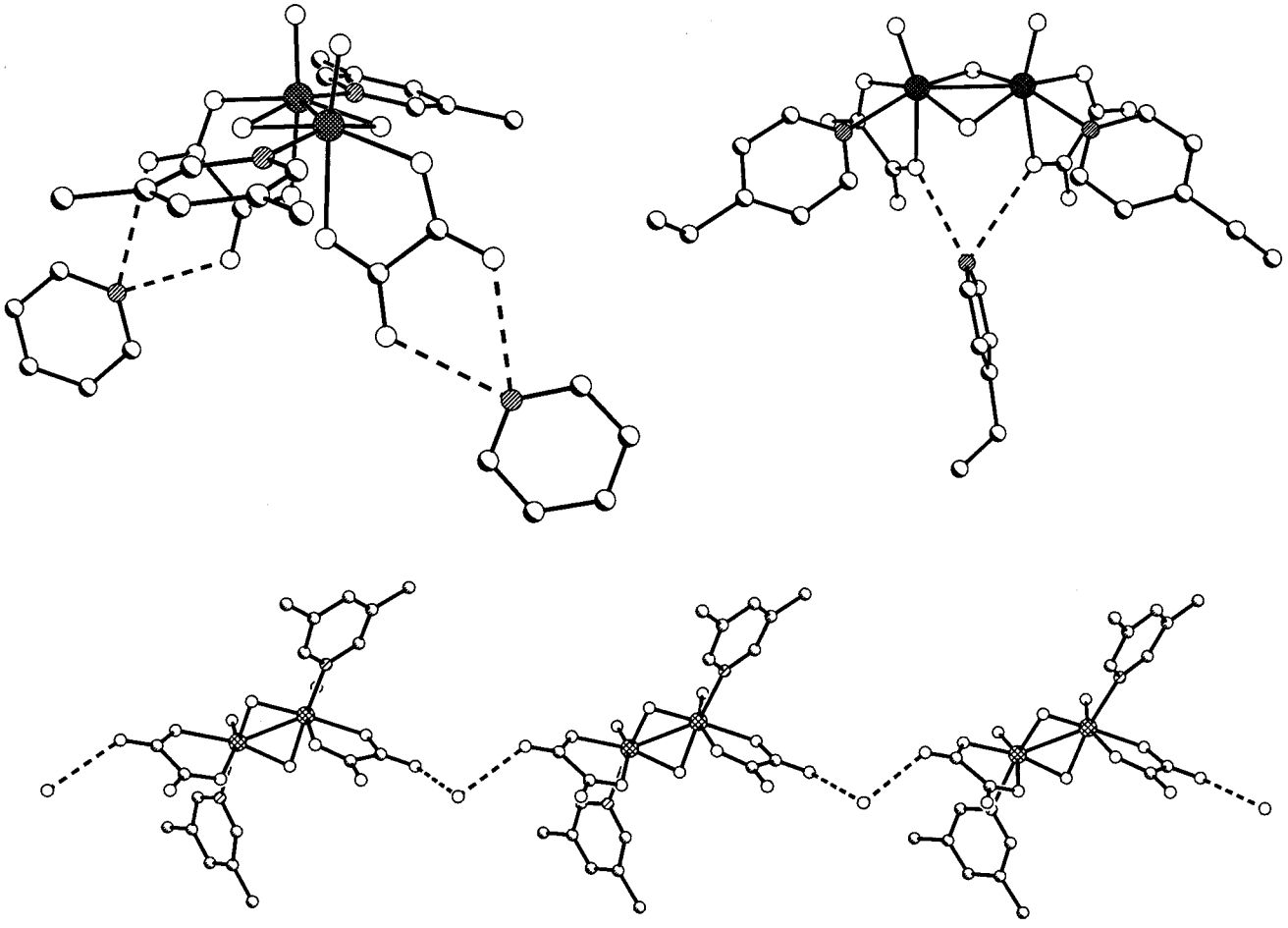

Figure 3. Types of hydrogen bonds in $[Mo_2O_4(\eta^2\text{-}C_2O_4)_2(R\text{-}Py)_2]^{2-}$ compounds.

contains two dinuclear anions and four pyridinium cations. The bonding pattern within the two crystallographically independent *trans*-$[Mo_2O_4(\eta^2\text{-}C_2O_4)_2(H_2O)_2]^{2-}$ anions is basically the same (see Table 3). Owing to the *trans* influence of the terminal oxo group, one of the two molybdenum-to-oxalate oxygen bond lengths is short and the other is long. The molybdenum-to-water bond lengths are comparable to those observed for $[Mo_4O_8(OH)_2(H_2O)_2(C_4O_4)_2]^{2-}$ [2.148(6) Å],[12] $Ba[Mo_2O_4(\eta^2\text{-}C_2O_4)_2(H_2O)_2]\cdot 3H_2O$ [2.198(4) Å], and $Cs_2[Mo_2O_4(\eta^2\text{-}C_2O_4)_2(H_2O)_2]\cdot H_2O$ [2.12(1) and 2.15(1) Å].[13,14]

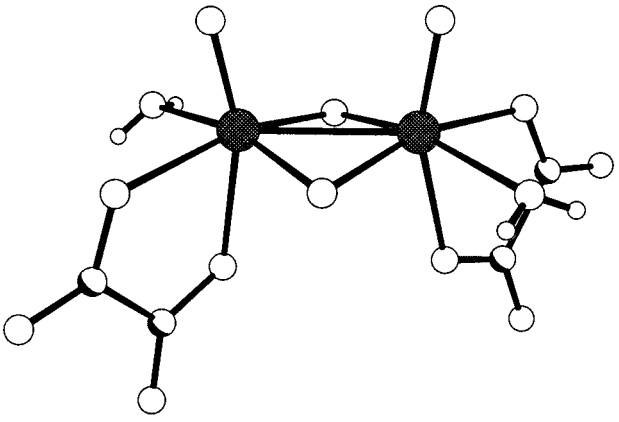

Figure 4. Drawing of the *trans*-$[Mo_2O_4(\eta^2\text{-}C_2O_4)_2(H_2O)_2]^{2-}$ anion in **8**.

Table 3. Selected geometric parameters [Å, °] for the *trans*-$[Mo_2O_4(\eta^2\text{-}C_2O_4)_2(H_2O)_2]^{2-}$ anion in **8**.[a]

Mo–O(oxalate)	Mo–Mo	Fold angle	Mo–O(water)
2.124(2) vs. 2.187(2)	2.5620(4)	153.6(1)	2.159(2)
			2.161(2)
2.143(2) vs. 2.164(2)			
2.115(2) vs. 2.197(2)	2.5626(4)	155.0(1)	2.160(2)
			2.150(2)
2.142(2) vs. 2.184(2)			

[a] Two sets of parameters are listed, one for each anion in the asymmetric unit.

A complicated pattern of hydrogen bonds is formed in **8**. Each water ligand forms two hydrogen bonds, one to the doubly-bridging oxo group of the adjacent anion, with O···O distances in the range 2.675(3)–2.720(3) Å, and one to the noncoordinated oxygen of the oxalate, also from the adjacent anion, with O···O distances in the range 2.643(3)–2.662(3) Å. Each anion forms a total of eight hydrogen bonds to four neighboring anions, two to each neighbor. Infinite layers that are coplanar with the (110) unit-cell plane are thus formed. Pyridinium cations are attached to the oxalate oxygen atoms on both sides of these layers through the agency of hydrogen bonds with lengths in the range 2.744(4)–3.125(5) Å.

The structure of the $[Mo_2O_4(\eta^2\text{-}C_2O_4)_2(H_2O)_2]^{2-}$ anion has been determined previously. It is of interest to note that the X-ray structure determination of *trans*-$Ba[Mo_2O_4(\eta^2\text{-}C_2O_4)_2(H_2O)_2]\cdot 3H_2O$ was also the first on a compound containing the $\{Mo_2O_4\}^{2+}$ unit and, as such, unambiguously confirmed the existence of the previously assumed $\{Mo_2O_4\}^{2+}$ structural core.[13] In contrast to the uniform tendency of Mo=O bonds to weaken bonds *trans* to themselves, no significant *trans* influence was observed. This phenomenon was ascribed to a low *trans* susceptibility of the oxalato ligand.[15] However, later structural determinations on the *trans*-$[Mo_2O_4(\eta^2\text{-}C_2O_4)_2(H_2O)_2]^{2-}$ anion clearly indicated the existence of a *trans* influence.[14] The pyridinium salt of this anion has also been reported, but with a different composition, $H(PyH)_3[Mo_2O_4(\eta^2\text{-}C_2O_4)_2(H_2O)_2]_2\cdot 2H_2O$.[16] In the case of the thio-bridged derivative of the dinuclear aqua-ligated anion, i.e., $[Mo_2O_2(\mu_2\text{-}S)_2(\eta^2\text{-}C_2O_4)_2(H_2O)_2]^{2-}$, the *cis* geometric isomer has been isolated as well. A *cis* arrangement of the ligands was observed in two caesium salts, *cis*-$KCs_3[Mo_2O_2S_2(\eta^2\text{-}C_2O_4)_2(H_2O)_2]_2\cdot 4H_2O$,[14] and *cis*-$NaCs_3[Mo_2O_2S_2(\eta^2\text{-}C_2O_4)_2(H_2O)_2]_2\cdot 6H_2O$.[17] These were the only known *cis* isomers prior to this study.

Structure of $(PyH)_2[Mo_8O_{16}(OCH_3)_8(\mu_8\text{-}C_2O_4)]\cdot 2CH_3OH$ (9)

Compound **9** crystallizes in a triclinic unit cell with one octanuclear anion $[Mo_8O_{16}(OCH_3)_8(\mu_8\text{-}C_2O_4)]^{2-}$, two protonated pyridine molecules as countercations, and two methanol molecules. The asymmetric unit consists of one half of the anion, with the other half generated by the inversion center located at the center of the ring. Each cyclic anion consists of four $\{Mo_2O_4\}^{2+}$ units arranged around the μ_8-oxalate and linked together by pairs of μ_2-bridging methoxides (Figure 5). The bonding pattern in the anion is very similar to that determined previously for $(Bu_4N)_2[Mo_8O_{16}(OCH_3)_8(\mu_8\text{-}C_2O_4)]$[18] and $(MeNC_5H_5)_2[Mo_8O_{16}(OCH_3)_8(\mu_8\text{-}C_2O_4)]$:[11] the Mo–Mo bonds are 2.5767(4)–2.5876(4) Å, the nonbonding Mo···Mo contacts

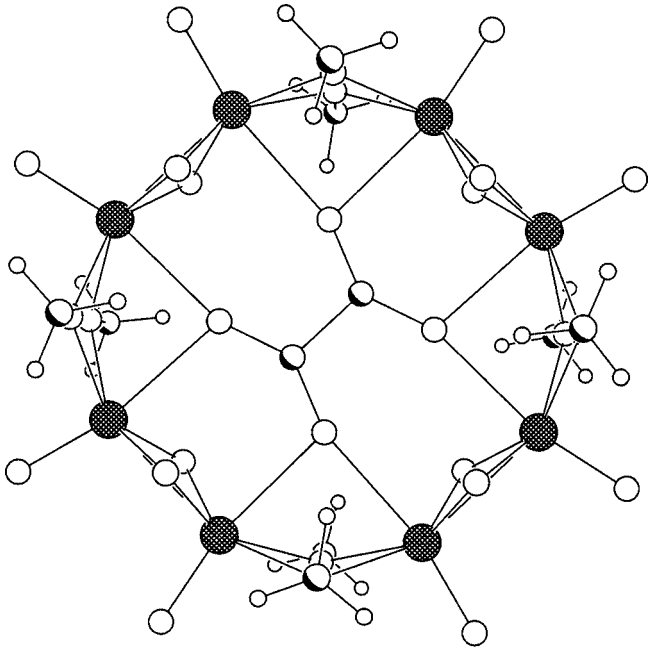

Figure 5. Drawing of the $[Mo_8O_{16}(OCH_3)_8(\mu_8\text{-}C_2O_4)]^{2-}$ anion in **9**.

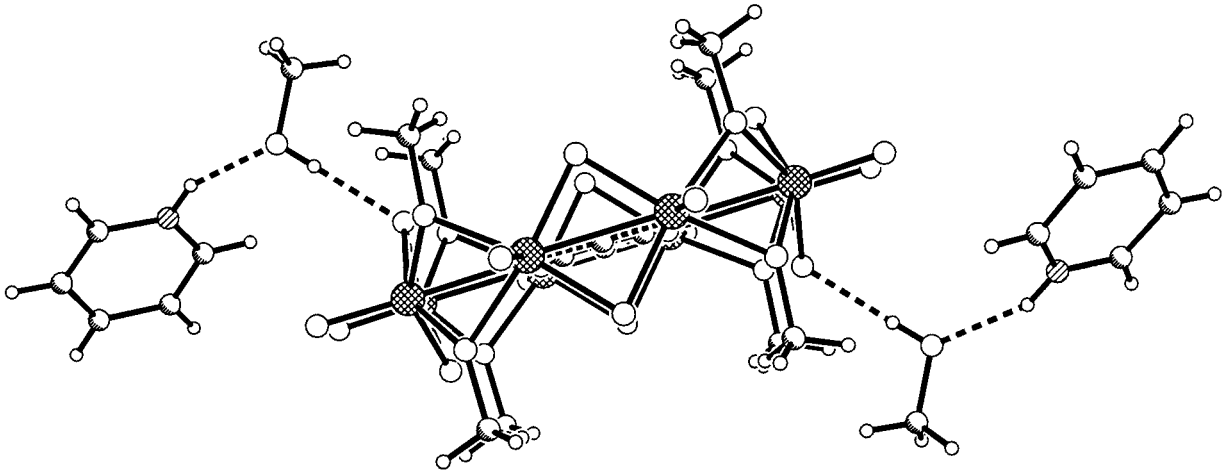

Figure 6. Octanuclear anion in **9** with a pair of hydrogen bonded methanol molecules and pyridinium cations.

spanning the methoxide bridges are 3.2489(4)–3.2548(4) Å, and the molybdenum-to-oxalate bond lengths are 2.357(3)–2.386(3) Å. Each octanuclear anion has a pair of methanol molecules linked by hydrogen bonds to the doubly-bridging oxo groups with lengths of 2.745(4) Å. Methanol participates in another hydrogen-bonding interaction with the protonated pyridine nitrogen, where it acts as the acceptor of the hydrogen bond (Figure 6). The corresponding O···N distance is 2.686(4) Å. Recently, a related octanuclear ring, $[Mo_8S_4O_{12}(OH)_8(C_2O_4)]^{2-}$, was reported. It is built of four $\{Mo_2O_2(\mu_2\text{-}O)(\mu_2\text{-}S)\}^{2+}$ subunits.[19] It supplements a series of octanuclear, cyclic anions built either of $\{Mo_2O_4\}^{2+}$ units or thio-bridged analogs, i.e., $\{Mo_2O_2(\mu_2\text{-}O)(\mu_2\text{-}S)\}^{2+}$ and $\{Mo_2O_2(\mu_2\text{-}S)_2\}^{2+}$.[17] This series confirms the ability of the structurally related, yet chemically markedly different, dinuclear cores to assemble in a similar manner with the formation of clusters with the same architectures. A structural similarity was observed with several other molybdenum(v) oxalato complexes, namely *trans*-$[Mo_2O_4(\eta^2\text{-}C_2O_4)_2(H_2O)_2]^{2-}$ and its thio analog *trans*-$[Mo_2O_2S_2(\eta^2\text{-}C_2O_4)_2(H_2O)_2]^{2-}$,[15,20] and a series of tetranuclear anions, i.e., $[\{Mo_2O_4(\eta^2\text{-}C_2O_4)_2\}_2(\mu_4\text{-}C_2O_4)]^{6-}$,[11] $[\{Mo_2O_3S(\eta^2\text{-}C_2O_4)_2\}_2(\mu_4\text{-}C_2O_4)]^{6-}$,[20,21] and $[\{Mo_2O_2S_2(\eta^2\text{-}C_2O_4)_2\}_2(\mu_4\text{-}C_2O_4)]^{6-}$.[17] It is of interest to note that the recently reported hexanuclear species $[\{Mo_2O_2S_2\}_3(OH)_4(\eta^2\text{-}C_2O_4)_2(\mu_6\text{-}C_2O_4)]^{4-}$ has only been observed for the $\{Mo_2O_2(\mu_2\text{-}S)_2\}^{2+}$ series of compounds.[22]

Synthetic Considerations

The basic reaction system inspected was that with a pyridine, oxalic acid, acetonitrile, an alcohol, and $(PyH)_5[MoOCl_4(H_2O)]_3Cl_2$ or $(PyH)[MoOBr_4]$. Both molybdenum starting materials possess labile sites (aqua and halo ligands), which in the mixtures of pyridine and methanol undergo a facile substitution chemistry with the formation of the $\{Mo_2O_4\}^{2+}$ structural unit or discrete clusters, as demonstrated before.[3] With a sufficient amount of oxalate, i.e. a ligand to metal ratio greater than 1, the formation of *trans*-$[Mo_2O_4(\eta^2\text{-}C_2O_4)_2Py_2]^{2-}$ takes place. The dinuclear anion was isolated in two salts, one with protonated pyridine molecules as countercations and the other as an *N*-methylpyridinium salt.[11] The two salts have different solubilities. While the pyridinium salt of *trans*-$[Mo_2O_4(\eta^2\text{-}C_2O_4)_2Py_2]^{2-}$ is only soluble in water, the *N*-methylpyridinium salt is also soluble in methanol. Contrary to our expectations, the *N*-alkylation of pyridine which occurs in the latter case did not turn out to be a general reaction:[23] it was observed only in the case of methanol. When other alcohols were used, such as ethanol, 2-propanol and *tert*-butanol, the only solid isolated was *trans*-$(PyH)_2[Mo_2O_4(\eta^2\text{-}C_2O_4)_2Py_2]$ (**1**). It is pertinent to note that the reaction mixture in the absence of alcohol also produced **1**. Although not required for the formation of dinuclear anions, the use of alcohols was justified by the fact that most oxalate salts, either with protonated or *N*-methylated pyridines, exhibit good alcohol solubility and the only product which crystallizes from the reaction mixture is that with the $[Mo_2O_4(\eta^2\text{-}C_2O_4)_2(R\text{-}Py)_2]^{2-}$ anion.

By using 4-methylpyridine in place of pyridine we hoped to prepare analogous compounds of *trans*-$[Mo_2O_4(\eta^2\text{-}C_2O_4)_2(4\text{-}MePy)_2]^{2-}$, which, provided they were also methanol soluble, would be a better choice for NMR solution studies as the anion $[Mo_2O_4(\eta^2\text{-}C_2O_4)_2(4\text{-}MePy)_2]^{2-}$ would not only display a simpler pattern of aromatic resonances than pyridine, but also a methyl singlet in a different spectral region which could serve as a probe for monitoring the substitution reactions. However, the reaction mixture described for the preparation of **6** afforded two crystalline phases whose identities were revealed by X-ray structure analyses as *trans*-$(4\text{-}MePyH)_2[Mo_2O_4(\eta^2\text{-}C_2O_4)_2(4\text{-}MePy)_2]\cdot 1/2(4\text{-}MePy)$ (**5**) and *cis*-$(4\text{-}MePyH)_3[Mo_2O_4(\eta^2\text{-}C_2O_4)_2(4\text{-}MePy)_2]Br$ (**6**). The described reaction shows that the formation of both isomeric forms of the $[Mo_2O_4(\eta^2\text{-}C_2O_4)_2(4\text{-}MePy)_2]^{2-}$ anion takes place simultaneously from the same reaction mixture, under the same conditions. MO calculations performed on the isomeric pair of $[Mo_2O_4(\eta^2\text{-}C_2O_4)_2(4\text{-}MePy)_2]^{2-}$ anions revealed insignificant differences in their energy. According to the most reliable approach of the three used, the B3LYP density functional with a 6-31G*

basis set and pseudopotential, the *trans* isomer of $[Mo_2O_4(\eta^2\text{-}C_2O_4)_2(4\text{-}MePy)_2]^{2-}$ has a lower energy than the corresponding *cis* isomer by only 7.24 kJ mol^{-1}. With so small an energy difference, the formation of either is equally probable unless the pair differs in solubility. The stereochemistry of the product thus depends to a larger extent upon its solubility rather than on the reaction conditions employed.

NMR Solution Studies

The ^{1}H NMR spectrum of an aqueous solution of *trans*-$(PyH)_2[Mo_2O_4(\eta^2\text{-}C_2O_4)_2Py_2]$ (**1**) recorded at room temperature reveals six broad resonances in the aromatic spectral region, indicating that the pyridine ligands are involved in an exchange process. The temperature-dependent nature of these reactions was confirmed by recording the spectra at higher temperatures, at 10 K intervals up to 343 K, where the six resonances coalesce into three [δ = 8.25 (2 H, 3-H), 8.74 (1 H, 4-H), and 9.20 ppm (2 H, 2-H)] and the signals corresponding to pyridine, in coordinated and free form, and pyridinium cation became indistinguishable. The NMR spectra of aqueous solutions of *trans*-$(4\text{-}MePyH)_2[Mo_2O_4(\eta^2\text{-}C_2O_4)_2(4\text{-}MePy)_2]\cdot 1/2(4\text{-}MePy)$ (**5**) and *cis*-$(4\text{-}MePyH)_3[Mo_2O_4(\eta^2\text{-}C_2O_4)_2(4\text{-}MePy)_2]Br$ (**6**) gave evidence for another process. Apart from different values of integrals due to differences in the composition of **5** and **6**, their spectra are the same: a set of broad resonances in the aromatic spectral region and two, also broadened, methyl resonances. The isomerization of the *cis* into the *trans* isomer and vice versa was assumed to take place. The use of methanol-soluble *trans*-$(MeNC_5H_5)_2[Mo_2O_4(\eta^2\text{-}C_2O_4)_2Py_2]$ enabled NMR experiments at temperatures below 273 K and a quantitative evaluation of this process. Since the *N*-methylpyridinium cation does not participate in the exchange process in the way the pyridinium cation does, its resonances (three in the aromatic part of the spectrum and the methyl singlet) are consequently sharp and their integrals remain constant. Upon lowering the temperature, the previously broad pyridine resonances become sharper and at 243 K are resolved into seven signals, shown by COSY to belong to three sets, denoted as A, B and C (Figure 7). The signals C2, C3, and C4 were unambiguously identified by the addition of a small amount of pyridine as belonging to free pyridine.[24] Its presence can be accounted for only if the complex is partially dissociated, but in that case, an additional set of signals belonging to the mono-substituted $[Mo_2O_4(\eta^2\text{-}C_2O_4)_2Py(H_2O)]^{2-}$ is expected. Two isomeric forms are also possible for the mono-substituted complex. Since the environments of pyridine ligands in both are very similar, we assume that the pair is indistinguishable in the ^{1}H NMR spectrum. Accordingly, the mono-substituted complex is considered throughout the text as one species only. The bis(aqua)-ligated $[Mo_2O_4(\eta^2\text{-}C_2O_4)_2(H_2O)_2]^{2-}$ is also present; however this species is invisible in the ^{1}H NMR spectrum. The remaining four signals belong to sets A and B. Only the resonances of 2,6-H protons were clearly separated (A2 doublet centered at δ = 9.30 ppm and B2 doublet centered at δ = 9.16 ppm), while the resonances of the 4-H and 3,5-H protons were superimposed on each other (A4, B4 and A3, B3 signals). It is reasonable to expect that the immediate coordination environment is mostly experienced by the 2,6-H pair and to a significantly smaller extent by the 4-H proton or the 3,5-H pair. Set A was therefore assigned to belong to coordinated pyridine ligands in *cis*-$[Mo_2O_4(\eta^2\text{-}C_2O_4)_2Py_2]^{2-}$ and set B to *trans*-$[Mo_2O_4(\eta^2\text{-}C_2O_4)_2Py_2]^{2-}$ and the mono-substituted $[Mo_2O_4(\eta^2\text{-}C_2O_4)_2Py(H_2O)]^{2-}$ together. This assignment was based on the values of integrals of signals A2, B2, and C2[25] and the fact that the environment of the pyridine ligands in the *trans* isomer differs significantly from that in the *cis* isomer and that the environment of pyridine in the mono-substituted complex resembles that in the *trans* isomer very closely. On the basis of the chemical shifts of sets A and B, one can assume that the protons will resonate at lower field when the two pyridine rings are placed close to each other, as in the case of the *cis* isomer. In order to provide experimental support for the above-described assignment, two additional experiments were performed at 243 K. The solution of *trans*-$(MeNC_5H_5)_2[Mo_2O_4(\eta^2\text{-}C_2O_4)_2Py_2]$ was divided into two aliquots, of which one was repeatedly diluted and the other was titrated with pyridine. An increase in the concentration of free pyridine upon dilution was paralleled with the gradual decrease of the amount of coordinated pyridine, as monitored by the sum of integrals of signals A2 and B2 relative to the integral of the cation (Figure S1). The relative heights of A2 and B2 changed as well: a gradual decrease in the integral of A2 was observed, while B2 remained virtually constant within this concentration range. The signal B2 became slightly deformed, indicating two overlapping resonances. The pyridine titration had the opposite effect: the signal A2 started to gain in intensity, while B2 remained constant (Figure S2). The total amount of coordinated pyridine increased upon pyridine titration. The sum of integrals of signals A2 and B2 gravitated towards the integral of the cation. It was also observed that even with large additions of pyridine, {0.254 mmol of pyridine per 0.0405 mmol of $[Mo_2O_4(\eta^2\text{-}C_2O_4)_2Py_2]^{2-}$; Figure S2, spectrum f} the dissociation of pyridine was not entirely suppressed. Assuming that the extent of dissociation of the second pyridine ligand is very small and the amount of bis(aqua) complex negligible, approximate amounts of the mono-substituted complex and both major species, *cis*-$[Mo_2O_4(\eta^2\text{-}C_2O_4)_2Py_2]^{2-}$ and *trans*-$[Mo_2O_4(\eta^2\text{-}C_2O_4)_2Py_2]^{2-}$, could be calculated. Under these conditions, an excess of pyridine and a temperature of 243 K, around 8% of dinuclear complex exists in the mono-substituted form, while the *cis* isomer of $[Mo_2O_4(\eta^2\text{-}C_2O_4)_2Py_2]^{2-}$ exceeds its *trans* isomer in concentration by a factor of 1.8.

With the expectation that the oxalate carbon resonances would provide extra information about the major species in the solution, the ^{13}C NMR spectra were recorded. Of the three coordination sites of each metal in the $\{Mo_2O_4\}^{2+}$ moiety, the two sites that are in the *cis* position to the Mo=O group may be denoted as the equatorial ones, and

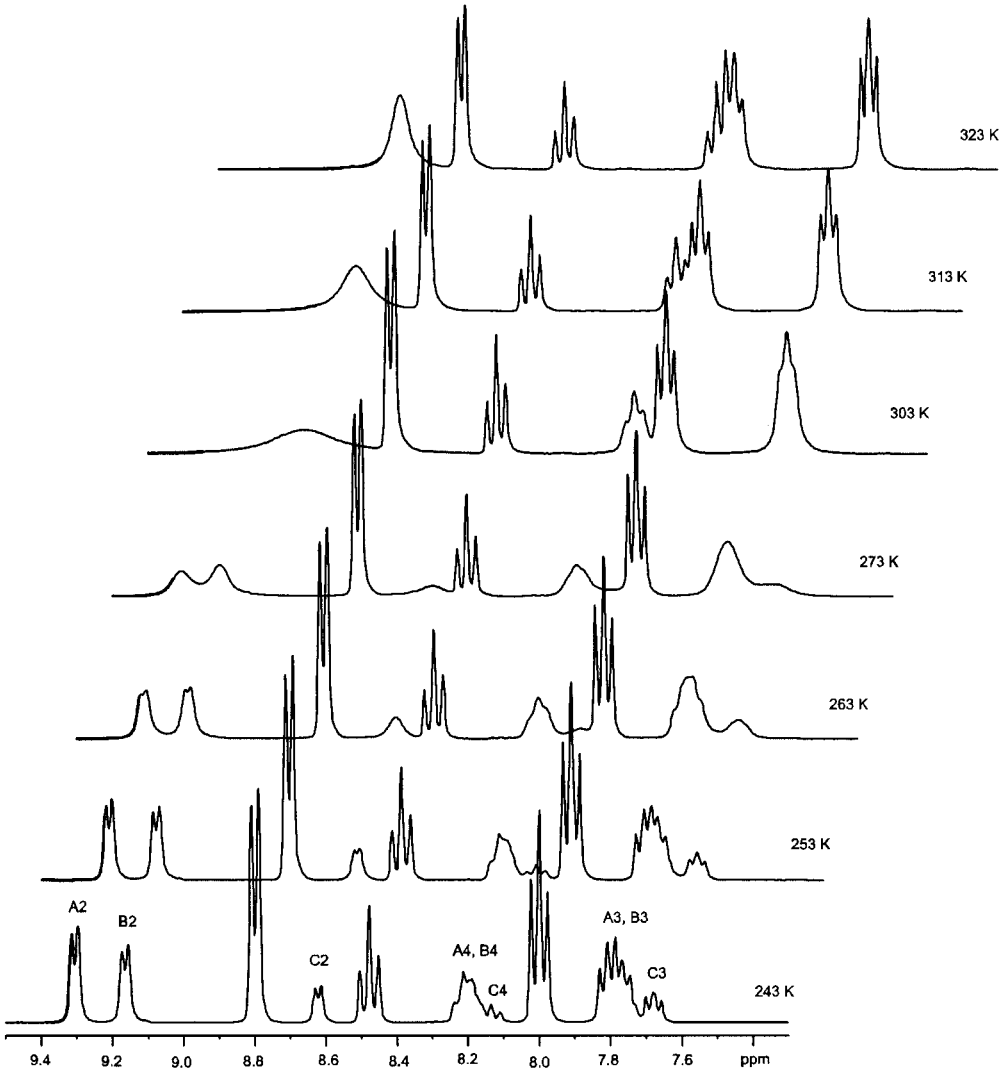

Figure 7. Variable temperature ^{1}H NMR spectra of *trans*-$(MeNC_5H_5)_2[Mo_2O_4(\eta^2\text{-}C_2O_4)_2Py_2]$. Labels A, B, and C refer to different pyridine species, and 2, 3, and 4 to pyridine protons 2,6, 3,5, and 4, respectively.

the remaining site, i.e. the one *trans* to the terminal oxo group, as the apical one. With the oxalate bonded in the bidentate manner as in the title compounds **1**–**8**, where one coordinated oxygen occupies the equatorial position and the other the apical position, the two oxalate carbon atoms are not chemically equivalent. Furthermore, the coordination environment of the oxalato ligand in *cis*-$[Mo_2O_4(\eta^2\text{-}C_2O_4)_2Py_2]^{2-}$ differs from that in *trans*-$[Mo_2O_4(\eta^2\text{-}C_2O_4)_2Py_2]^{2-}$. The room temperature ^{13}C NMR spectrum of *trans*-$(MeNC_5H_5)_2[Mo_2O_4(\eta^2\text{-}C_2O_4)_2Py_2]$ reveals two broad resonances at δ = 165.7 and 166.9 ppm, which resolved upon cooling to 243 K into three major ones at δ = 166.2, 166.5, and 167.7 ppm, and a minor one at δ = 167.5 ppm. However, no signal appeared at around δ = 173 ppm that would suggest the presence of free, noncoordinated oxalate.[26] In order to establish the dependence of the carbon oxalate frequencies upon the oxalate coordination mode, the ^{13}C NMR spectrum of $(MeNC_5H_5)_6[\{Mo_2O_4(\eta^2\text{-}C_2O_4)_2\}_2(\mu_4\text{-}C_2O_4)]$ was recorded. The oxalato ligands in the latter complex are bonded differently than in compounds **1**–**8** (Figure 8). Each of the four bidentate oxalates is bonded with both oxygen atoms in *cis* positions relative to the molybdenyl group, causing the chemical equivalence of the two carbon atoms. The carbon atoms of the tetraunidentate oxalate are equivalent as well. The ^{13}C NMR spectrum of $(MeNC_5H_5)_6[\{Mo_2O_4(\eta^2\text{-}C_2O_4)_2\}_2(\mu_4\text{-}C_2O_4)]$ reveals two resonances that could be associated with the oxalate moiety, an intense one at δ = 166.6 ppm and a weak one at δ = 173.0 ppm. The latter confirms the presence of free oxalate as a consequence of the rupture of the tetranuclear structure in solution. This result is not surprising in view of the results of the X-ray diffraction analysis, which showed that the bonds to μ_4-oxalate are weakened due to the labilizing *trans* influence of the four terminal oxo groups.[11] The cleavage of the tetranuclear anion produces two dinuclear $[Mo_2O_4(C_2O_4)_2]^{2-}$ fragments, each of which possesses two vacant coordination sites. Addition of one equivalent of pyridine per molybdenum results in a solution whose ^{1}H and ^{13}C NMR spectra are identical to the spectra of *trans*-$(MeNC_5H_5)_2[Mo_2O_4(\eta^2\text{-}C_2O_4)_2Py_2]$, differing only in the

ratios between the *N*-methylpyridinium cation and pyridine. Since the bidentate oxalato ligands in *trans*-$[Mo_2O_4(\eta^2\text{-}C_2O_4)_2Py_2]^{2-}$ and in $[\{Mo_2O_4(\eta^2\text{-}C_2O_4)_2\}_2(\mu_4\text{-}C_2O_4)]^{6-}$ do not occupy the same coordination sites of the $\{Mo_2O_4\}^{2+}$ unit, the equivalence of the NMR spectra indicates rearrangements on the sites occupied by the oxalates as well. The conversion of one isomer into another presumably proceeds via a five-coordinate intermediate state (Scheme 1). The intermediate species in which the bidentate oxalate is coordinated to the two equatorial sites and the free apical position remains to be occupied with a unidentate ligand, i.e. pyridine or water, is also probable. Its relative instability may be explained in terms of the *trans* influence of the terminal oxo group: it is more favorable if the apical position, which is subject to the *trans* influence, is occupied by one terminus of the bidentate ligand rather than by a unidentate ligand. Binding of pyridine to the apical position is therefore weaker and the ligand exchange at this position too fast, even at low temperatures, to be observed in the NMR spectrum. The dissociation of coordinated pyridine as the rate-determining step of the whole process was confirmed by measuring the rates of exchange in the 253–293 K temperature interval in the ^{1}H NMR spectra of $[Mo_2O_4(\eta^2\text{-}C_2O_4)_2Py_2]^{2-}$ prepared in situ. The rate constants were measured on the basis of the line broadening of signal A2, which belongs to the pyridine ligands of *cis*-$[Mo_2O_4(\eta^2\text{-}C_2O_4)_2Py_2]^{2-}$.[27] The shape of signal A2 at each temperature was compared with the corresponding signal in the simulated spectrum. The activation parameters for the dissociation of pyridine from *cis*-$[Mo_2O_4(\eta^2\text{-}C_2O_4)_2Py_2]^{2-}$ were calculated from Eyring plot (Figure 9): $\Delta H^{\ddagger} = 82 \pm 4$ kJ mol^{-1} and $\Delta S^{\ddagger} = 79 \pm 14$ J mol^{-1} K^{-1}. The positive activation entropy is in agreement with the proposed dissociative mechanism. The determined value of the activation enthalpy could serve as a rough estimate of the molybdenum-to-pyridine bond strength.

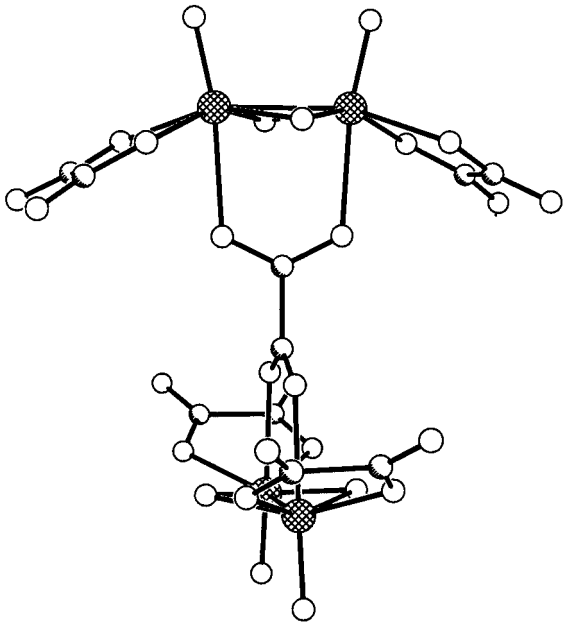

Figure 8. Oxalato ligands in $[\{Mo_2O_4(\eta^2\text{-}C_2O_4)_2\}_2(\mu_4\text{-}C_2O_4)]^{6-}$ adopt two binding modes: (i) the bidentate oxalates occupy the equatorial positions of the $\{Mo_2O_4\}^{2+}$ moiety, and (ii) the μ_4-oxalate occupies the apical positions of two $\{Mo_2O_4\}^{2+}$ moieties.[11]

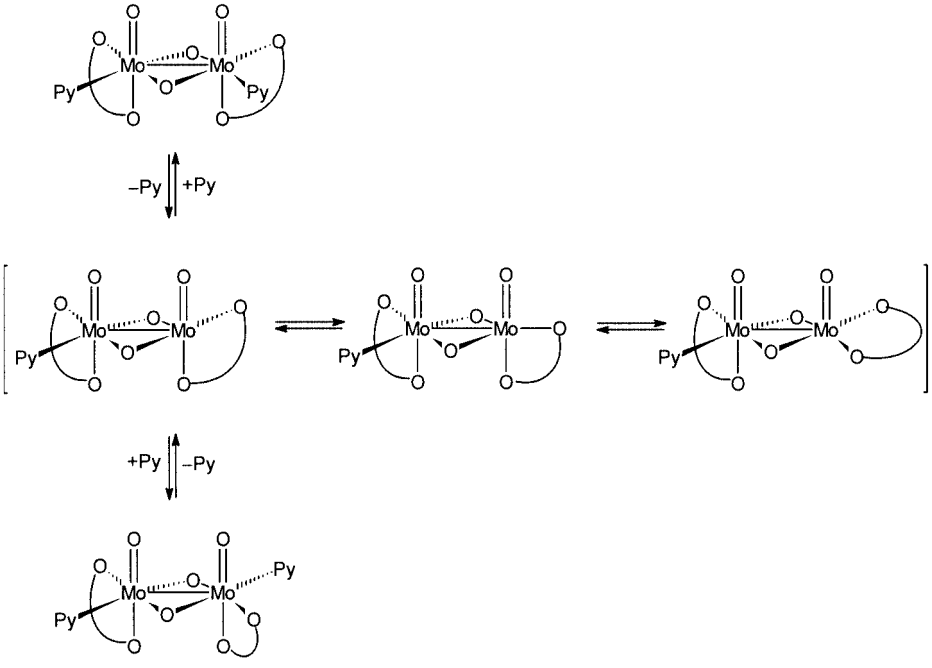

Scheme 1. Proposed *cis*/*trans* isomerization of $[Mo_2O_4(\eta^2\text{-}C_2O_4)_2Py_2]^{2-}$ with intermediate states included in square brackets. For simplicity, only the rearrangements on one metal center of the dinuclear anion are shown.

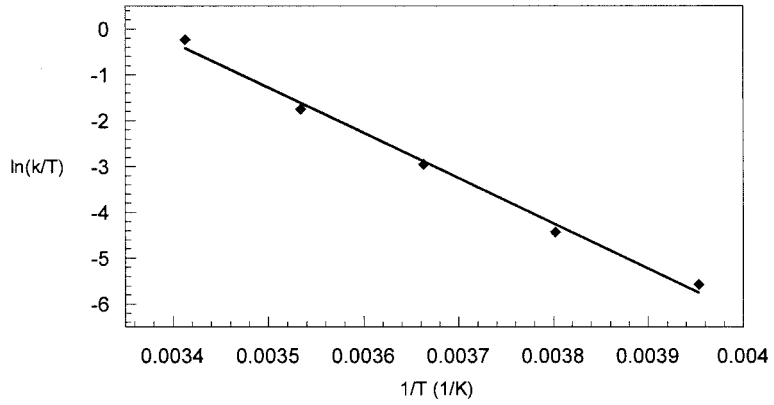

Figure 9. Eyring plot in the 253–293 K interval for the dissociation of pyridine from *cis*-$[Mo_2O_4(\eta^2\text{-}C_2O_4)_2Py_2]^{2-}$ in D_2O/CD_3OD solution. The solid line represents the equation $y = -9876 \cdot x + 33.284$ ($r^2 = 0.9934$) from the linear regression analysis.

Speculations on the Solution Chemistry of *cis*- and *trans*-$[Mo_2O_4(\eta^2\text{-}C_2O_4)_2(R\text{-}Py)_2]^{2-}$

Reports of oxalato complexes of molybdenum(v) date back almost a century, when the preparations of barium, potassium, and pyridinium salts of *trans*-$[Mo_2O_4(\eta^2\text{-}C_2O_4)_2(H_2O)_2]^{2-}$ were reported.[28] In a later study, the substitution chemistry of *trans*-$[Mo_2O_4(\eta^2\text{-}C_2O_4)_2(H_2O)_2]^{2-}$ with several ligands, including pyridine, was explored.[29] It was observed that the addition of pyridine to the sodium salt of *trans*-$[Mo_2O_4(\eta^2\text{-}C_2O_4)_2(H_2O)_2]^{2-}$ did not result in the coordination of pyridine; rather, the coordination sphere remained intact and the product was the pyridinium salt of the same anion. The substitution of water for pyridine in *trans*-$[Mo_2O_4(\eta^2\text{-}C_2O_4)_2(H_2O)_2]^{2-}$ was reported to be slow, with the equilibrium favoring the aqua complex. $(PyH)_2[Mo_2O_4(\eta^2\text{-}C_2O_4)_2Py_2]$ could only be prepared from $(PyH)_2[Mo_2O_4(\eta^2\text{-}C_2O_4)_2(H_2O)_2]$ upon prolonged refluxing in boiling pyridine. In reactions with some other ligands two other processes were suggested: a rupture of the doubly oxo-bridged structure to afford a singly oxo-bridged $\{Mo_2O_2(\mu_2\text{-}O)\}^{4+}$, and a substitution of the bidentate oxalate. Since the stereochemistry of the starting material was not known, no isomerization processes were proposed.

In line with the previous findings, we observed that both geometric isomers of $[Mo_2O_4(\eta^2\text{-}C_2O_4)_2(R\text{-}Py)_2]^{2-}$ react in water with the substitution of coordinated pyridine for water molecules, which are present in huge excess. This substitution is, as evidenced by NMR spectroscopy, accompanied by another process, namely isomerization of the *trans* isomer into the *cis* and vice versa. The crystallization of *trans*-$(PyH)_2[Mo_2O_4(\eta^2\text{-}C_2O_4)_2(H_2O)_2]$ (**8**) from a water/methanol solution of *cis*-$(4\text{-}EtPyH)_2[Mo_2O_4(\eta^2\text{-}C_2O_4)_2(4\text{-}EtPy)_2]$ (**4**) after the addition of pyridinium sulfate adds firm support for both processes. Slow evaporation of a solution of *trans*-$(PyH)_2[Mo_2O_4(\eta^2\text{-}C_2O_4)_2Py_2]$ (**1**) also afforded a dinuclear species with coordinated water – *trans*-$(PyH)_2[Mo_2O_4(\eta^2\text{-}C_2O_4)_2(H_2O)_2]$ (**8**). On the other hand, when the pyridinium cations in the solution of *trans*-$(PyH)_2[Mo_2O_4(\eta^2\text{-}C_2O_4)_2Py_2]$ (**1**) were neutralized with a strong base, followed by the addition of tetraphenylphosphonium bromide, no substitution occurred. The product was a water solvate – *trans*-$[(C_6H_5)_4P]_2[Mo_2O_4(\eta^2\text{-}C_2O_4)_2Py_2]\cdot H_2O$ (**7**) – which retains the original, *trans*, configuration of the ligands. Although water solutions of $[Mo_2O_4(\eta^2\text{-}C_2O_4)_2Py_2]^{2-}$ contain isomeric pairs of $[Mo_2O_4(\eta^2\text{-}C_2O_4)_2Py_2]^{2-}$, partially substituted $[Mo_2O_4(\eta^2\text{-}C_2O_4)Py(H_2O)]^{2-}$ and fully substituted, aqua-ligated $[Mo_2O_4(\eta^2\text{-}C_2O_4)_2(H_2O)_2]^{2-}$, we were not able either to isolate any of the two isomeric forms of $[Mo_2O_4(\eta^2\text{-}C_2O_4)_2Py(H_2O)]^{2-}$ or carry out the transformation of *trans*-$[Mo_2O_4(\eta^2\text{-}C_2O_4)_2Py_2]^{2-}$ into the *cis* isomeric form on a preparative scale.

In the context of the above-discussed reactions of $[Mo_2O_4(\eta^2\text{-}C_2O_4)_2Py_2]^{2-}$ anions in water, the reaction of *trans*-$(PyH)_2[Mo_2O_4(\eta^2\text{-}C_2O_4)_2(H_2O)_2]$ (**8**) with methanol has to be briefly mentioned. Although **8** is sparingly soluble in methanol, it slowly reacts with it. Evaporation of a lightly colored, saturated methanol solution yields orange crystals of $(PyH)_2[Mo_8O_{16}(OCH_3)_8(\mu_8\text{-}C_2O_4)]\cdot 2CH_3OH$ (**9**). The formation of this octanuclear anion supports several other processes. The coordinated oxalate is shown to be labile under certain conditions and can be substituted with other ligands, methoxide being such a ligand. Due to the rupture of the molybdenum-to-oxalate bonds, the oxalate content in the resulting species is greatly reduced. Since the variable temperature NMR studies were carried out in a water/methanol mixture, the formation of **9** shows that the role of methanol is not restricted solely to that of a solvent.

Vibrational Spectroscopy

The most relevant feature of the IR spectra of the title compounds concerns the carbon-oxygen frequencies of the oxalato ligand because they are diagnostic of its coordination mode.[30] Several absorption bands observed for ν_{as}(OCO) in the range 1710–1633 cm^{-1}, two bands for ν_s(OCO) in the range 1418–1249 cm^{-1}, and a single band for δ(OCO) at 789–780 cm^{-1} (see Table 4) are typical for the bidentate coordination mode found in complexes **1**–**8**. The observed frequencies agree very well with the data observed for $Ba[Mo_2O_4(\eta^2\text{-}C_2O_4)_2(H_2O)_2]\cdot 3H_2O$ {1710, 1680, 1653 [ν_{as}(OCO)], 1430, 1289 [ν_s(OCO)], 793 [δ(OCO)]}.[13] For

the anion in **9** with all oxalate oxygen atoms engaged in coordination and metal–oxygen distances of approximately equal length, bands at 1661, 1650 [ν_{as}(OCO)], 1389, 1283 [ν_s(OCO)], and 814 [δ(OCO)] cm^{-1} were observed. Their frequencies do not differ from those reported for the *N*-methylpyridinium salt of this anion.[11]

Table 4. Characteristic oxalate absorptions [cm^{-1}] in $[Mo_2O_4(\eta^2\text{-}C_2O_4)_2(R\text{-}Py)_2]^{2-}$ compounds and in *trans*-$(PyH)_2[Mo_2O_4(\eta^2\text{-}C_2O_4)_2(H_2O)_2]$ (**8**).

Compound	ν_{as}(OCO)	ν_s(OCO)	δ(OCO)
1	1707, 1681, 1638	1418, 1279	789
2	1707, 1671	1415, 1275	780
3	1710, 1662	1376, 1294	785
4	1708, 1669, 1634	1417, 1272	785
5	1709, 1667	1414, 1275	784
6	1707, 1682, 1633	1417, 1277	789
7	1707, 1687, 1672	1376, 1249	784
8	1650[a]	1392, 1287	788

[a] A single, very broad band is displayed. The water bending mode absorbs in the same spectral region.

The antisymmetric and symmetric O–H stretching modes of the lattice water in **3** appear at 3533 and 3464 cm^{-1}, and in **7** at 3526 and 3396 cm^{-1}. Their frequencies fall in the usually observed region (3550–3200 cm^{-1}).[31] The absorptions assigned to coordinated water in the spectrum of **8** are seen as very broad bands. A broad band centered at about 2900 cm^{-1} may be attributed to both types of O–H stretching vibrations. The typical region for the water bending vibration (1630–1600 cm^{-1})[31] overlaps with the ν_{as}(OCO) vibration of the oxalate.

Conclusions

A series of compounds containing the *trans* or *cis* isomeric form of the $[Mo_2O_4(\eta^2\text{-}C_2O_4)_2(R\text{-}Py)_2]^{2-}$ anion has been prepared. *trans*-$(4\text{-}MePyH)_2[Mo_2O_4(\eta^2\text{-}C_2O_4)_2(4\text{-}MePy)_2]\cdot 1/2(4\text{-}MePy)$ (**5**) and *cis*-$(4\text{-}MePyH)_3[Mo_2O_4(\eta^2\text{-}C_2O_4)_2(4\text{-}MePy)_2]Br$ (**6**) are the only examples where both isomers were isolated. The stepwise substitution of pyridine for water in solutions of $[Mo_2O_4(\eta^2\text{-}C_2O_4)_2Py_2]^{2-}$ produces the mono-substituted $[Mo_2O_4(\eta^2\text{-}C_2O_4)_2Py(H_2O)]^{2-}$, whose presence was detected by NMR spectroscopy, and the bis-(aqua)-ligated $[Mo_2O_4(\eta^2\text{-}C_2O_4)_2(H_2O)_2]^{2-}$. The isolation of *trans*-$(PyH)_2[Mo_2O_4(\eta^2\text{-}C_2O_4)_2(H_2O)_2]$ (**8**) from a solution of *cis*-$(4\text{-}EtPyH)_2[Mo_2O_4(\eta^2\text{-}C_2O_4)_2(4\text{-}EtPy)_2]$ (**4**) adds firm support for simultaneous *cis*/*trans* isomerization accompanying the substitution reactions. The latter result is in accordance with the MO calculations on the *trans* and *cis* isomer of $[Mo_2O_4(\eta^2\text{-}C_2O_4)_2(4\text{-}MePy)_2]^{2-}$, which revealed insignificant differences in their energy.

Experimental Section

General Remarks: Reagents were purchased from Aldrich and used without further purification. $(PyH)_5[MoOCl_4(H_2O)]_3Cl_2$ and $(PyH)[MoOBr_4]$ were prepared by published procedures.[32,33] Pyridinium sulfate was isolated as a white solid by neutralizing sulfuric acid with two equiv. of pyridine and drying in vacuo. The solvothermal reactions were carried out in sealed glass tubes under autogenous pressure. Several synthetic procedures are described for some compounds. The IR and far-IR spectra were measured on solid samples as Nujol or poly(chlorotrifluoroethylene) mulls using Perkin–Elmer 2000 series FT-IR spectrometer. ^1H and ^{13}C spectra were recorded on a Bruker Avance DPX 300 spectrometer referenced to the solvent. Elemental analyses were performed by the Chemistry Department service at the University of Ljubljana. The compounds **1**, **2**, **4**, and **6** were found to decompose on prolonged exposure to the air.

NMR Spectroscopy of *trans*-$(MeNC_5H_5)_2[Mo_2O_4(\eta^2\text{-}C_2O_4)_2Py_2]$: *trans*-$(MeNC_5H_5)_2[Mo_2O_4(\eta^2\text{-}C_2O_4)_2Py_2]$ (63 mg, 0.0809 mmol), prepared following the previously published procedure,[11] was dissolved in 0.6 mL of D_2O/CD_3OD mixture (1:1 volume ratio). The variable temperature ^1H NMR spectra (the aromatic region) are shown in Figure 7. The signals for the *N*-methylpyridinium cation in the spectrum recorded at 243 K are at δ = 4.36 (s, 3 H, $CH_3NC_5H_5$), 8.00 (m, 2 H, 3-H), 8.48 (t, J = 7.8 Hz, 1 H, 4-H), and 8.80 (d, J = 5.9 Hz, 2 H, 2-H) ppm. The assignments of other signals are described in the text.

NMR Spectroscopy of $(MeNC_5H_5)_6[\{Mo_2O_4(\eta^2\text{-}C_2O_4)_2\}_2(\mu_4\text{-}C_2O_4)]$: $(MeNC_5H_5)_6[\{Mo_2O_4(\eta^2\text{-}C_2O_4)_2\}_2(\mu_4\text{-}C_2O_4)]$ was prepared following the previously published procedure.[11] ^1H NMR (D_2O, 300 MHz): δ = 4.35 (s, 3 H, $CH_3NC_5H_5$), 8.00 (m, 2 H, 3-H), 8.48 (t, J = 7.9 Hz, 1 H, 4-H), 8.73 (d, J = 5.9 Hz, 2 H, 2-H) ppm. ^{13}C NMR (D_2O, 75 MHz): δ = 48.5 ($CH_3NC_5H_5$), 128.4 (C-3), 145.4 (C-2), 145.6 (C-4), 166.6 (coordinated oxalate), 173.0 (free oxalate) ppm.

NMR Determination of the Exchange Rates: $(MeNC_5H_5)_6[\{Mo_2O_4(\eta^2\text{-}C_2O_4)_2\}_2(\mu_4\text{-}C_2O_4)]$ (22 mg, 14.5 mmol) was dissolved in D_2O (0.3 mL), followed by the addition of CD_3OD (0.3 mL). An excess of pyridine (15.4 mg, 0.1927 mmol) was added to this solution. The relative amounts of *cis*-$[Mo_2O_4(\eta^2\text{-}C_2O_4)_2Py_2]^{2-}$, *trans*-$[Mo_2O_4(\eta^2\text{-}C_2O_4)_2Py_2]^{2-}$, and $[Mo_2O_4(\eta^2\text{-}C_2O_4)_2Py(H_2O)]^{2-}$ were calculated from the integrals of the corresponding signals. The spectra were measured at 10 K intervals in the temperature range 233–333 K.

***trans*-$(PyH)_2[Mo_2O_4(\eta^2\text{-}C_2O_4)_2Py_2]$ (1):** A glass tube was charged with $(PyH)_5[MoOCl_4(H_2O)]_3Cl_2$ (50 mg, 0.117 mmol of Mo), $H_2C_2O_4\cdot 2H_2O$ (20 mg, 0.159 mmol), acetonitrile (0.5 mL), *tert*-butanol (1 mL), and pyridine (4 mL). The tube was sealed and heated for 90 h in an electric oven maintained at 115 °C. The tube was then allowed to cool slowly to room temperature. Orange, block-shaped crystals of **1** were collected by filtration and washed with dichloromethane. Yield: 73% (32 mg). *Note.* Other alcohols (ethanol, 2-propanol) can be used instead of *tert*-butanol. The yields are comparable (77% for the reaction mixture with ethanol and 80% for the reaction mixture with 2-propanol). IR: $\tilde{\nu}$ = 3130 cm^{-1} (w), 3089 (w), 3053 (w), 2168 (w), 2066 (w), 1707 (vvs), 1681 (vvs), 1638 (vvs), 1542 (vs), 1487 (vvs), 1418 (vvs), 1279 (vvs), 1224 (vs), 1203 (vs), 1171 (w), 1137 (w), 1078 (m), 1046 (m), 1016 (m), 997 (m), 955 (vvs), 935 (vs), 907 (s), 789 (vvs), 773 (vvs), 760 (vs), 742 (vvs), 691 (vvs), 641 (m), 603 (vs), 528 (s), 491 (vs), 477 (s), 441 (m), 400 (m), 361 (s), 341 (w), 318 (s), 291 (w), 279 (w), 269 (m), 247 (m), 228 (w) cm^{-1}. $C_{24}H_{22}Mo_2N_4O_{12}$ (750.3): calcd. C 38.42, H 2.96, N 7.47; found C 38.18, H 2.99, N 7.30.

***trans*-$(PyH)_2[Mo_2O_4(\eta^2\text{-}C_2O_4)_2(3,5\text{-}Lut)_2]$ (2):** $(PyH)_5[MoOCl_4(H_2O)]_3Cl_2$ (200 mg, 0.466 mmol of Mo) and $H_2C_2O_4\cdot 2H_2O$ (200 mg, 1.59 mmol) were added to a mixture of 3,5-lutidine (2 cm^3), methanol (2.5 mL), and acetonitrile (0.5 mL) in an Erlenmeyer flask. The reaction mixture was allowed to stand in the

closed flask under ambient conditions for ten days. Orange crystals of **2** were collected by filtration and washed with dichloromethane. Yield: 24% (45 mg). IR: $\tilde{\nu}$ = 3061 cm^{-1} (w), 1707 (vvs), 1671 (vvs), 1604 (s), 1595 (s), 1523 (s), 1482 (vs), 1415 (vs), 1325 (w), 1275 (vvs), 1248 (w), 1198 (m), 1169 (w), 1153 (vvs), 1093 (w), 1044 (m), 1022 (m), 1003 (m), 952 (vvs), 938 (vs), 907 (s), 875 (m), 780 (vvs), 768 (vvs), 740 (vvs), 705 (s), 694 (vs), 637 (w), 608 (m), 540 (w), 529 (m), 489 (vs), 480 (s), 430 (w), 397 (m), 363 (s), 345 (m), 317 (s), 256 (s) cm^{-1}. $C_{28}H_{30}Mo_2N_4O_{12}$ (806.4): calcd. C 41.70, H 3.75, N 6.95, found C 41.49, H 3.86, N 6.82.

***trans*-[$MeNC_5H_3(Me)_2]_2[Mo_2O_4(\eta^2\text{-}C_2O_4)_2$(3,5-Lut)$_2]\cdot H_2O$ (3):** A glass tube was charged with (PyH)[$MoOBr_4$] (120 mg, 0.235 mmol), $H_2C_2O_4\cdot 2H_2O$ (100 mg, 0.794 mmol), tetraphenylphosphonium bromide (100 mg, 0.239 mmol), 3,5-lutidine (4 mL), methanol (0.5 mL), and acetonitrile (0.5 mL). The tube was sealed and heated for 90 h in an electric oven maintained at 115 °C. The reaction mixture was then allowed to cool slowly to room temperature. Orange, block-like crystals of **3** were separated manually from unidentified crystalline material of a light yellow color, probably the *N*-methyl-3,5-lutidinium salt of oxalic acid. Yield: 49% (52 mg). IR: $\tilde{\nu}$ = 3533 cm^{-1} (w), 3464 (w), 1710 (vvs), 1662 (vvs), 1376 (s), 1307 (s), 1294 (s), 1254 (vs), 1215(w), 1205(m), 1185 (m), 1153 (s), 1052 (m), 1039 (m), 1028 (m), 943 (vvs), 923 (vs), 899 (vs), 867 (s), 785 (vs), 772 (vs), 739 (vs), 724 (vs), 699 (m), 677 (vs), 612 (w), 588 (w), 525 (m), 474 (vs), 416 (w), 397 (m), 353 (m), 314 (s), 296 (w), 277 (m), 261 (w) cm^{-1}. $C_{34}H_{44}Mo_2N_4O_{13}$ (908.6): calcd. C 44.95, H 4.88, N 6.17, found C 44.87, H 4.69, N 6.03.

***cis*-(4-EtPyH)$_2$[$Mo_2O_4(\eta^2\text{-}C_2O_4)_2$(4-EtPy)$_2$] (4). Procedure a:** A glass tube was charged with $(PyH)_5[MoOCl_4(H_2O)]_3Cl_2$ (50 mg, 0.117 mmol of Mo), $H_2C_2O_4\cdot 2H_2O$ (20 mg, 0.159 mmol), and 4-ethylpyridine (3 mL). The tube was sealed and heated for 90 h in an electric oven maintained at 115 °C. The tube was then allowed to cool slowly to room temperature. Large, orange, plate-like crystals of **4** were collected by filtration and washed with dichloromethane. Yield: 79% (40 mg). **Procedure b:** A glass tube was charged with (PyH)[$MoOBr_4$] (75 mg, 0.147 mmol), $H_2C_2O_4\cdot 2H_2O$ (20 mg, 0.159 mmol), 4-ethylpyridine (3 mL), 2-propanol (0.5 mL), and acetonitrile (0.5 mL). The tube was sealed and heated for 90 h in an electric oven maintained at 115 °C. The tube was then allowed to cool slowly to room temperature. Large, orange, plate-like crystals of **4** were collected by filtration and washed with dichloromethane. Yield: 82% (52 mg). IR: $\tilde{\nu}$ = 3068 cm^{-1} (w), 2922 (m), 2851 (m), 1708 (s), 1669 (vs), 1634 (vs), 1615 (vs), 1495 (m), 1455 (w), 1417 (s), 1314 (w), 1272 (m), 1224 (w), 1201 (m), 1108 (w), 1066 (m), 1028 (m), 946 (vvs), 930 (s), 904 (m), 833 (vs), 785 (vs), 740 (vs), 720 (m), 662 (w), 647 (w), 580 (w), 560 (w), 521 (w), 486 (s), 404 (w), 362 (m), 347 (w), 313 (s), 285 (w), 273 (w), 254 (m) cm^{-1}. $C_{32}H_{38}Mo_2N_4O_{12}$ (862.5): calcd. C 44.56, H 4.44, N 6.50, found C 44.34, H, 4.38, N, 6.41.

***trans*-(4-MePyH)$_2$[$Mo_2O_4(\eta^2\text{-}C_2O_4)_2$(4-MePy)$_2$]·1/2(4-MePy) (5):** A glass tube was charged with $(PyH)_5[MoOCl_4(H_2O)]_3Cl_2$ (50 mg, 0.117 mmol of Mo), $H_2C_2O_4\cdot 2H_2O$ (50 mg, 0.397 mmol), 4-methylpyridine (4 mL), 2-propanol (0.5 mL), and acetonitrile (0.5 mL). The tube was sealed and heated for 90 h in an electric oven maintained at 115 °C. The tube was then allowed to cool slowly to room temperature. Yellow, needle-shaped crystals of **5** were collected by filtration. Yield (based on the dried sample): 32% (15 mg). IR: $\tilde{\nu}$ = 3512 cm^{-1} (w), 3416 (w), 3062 (m), 1709 (vvs), 1667 (vvs), 1501 (vvs), 1462 (vvs), 1414 (vs), 1306 (w), 1275 (s), 1230 (m), 1212 (m), 1200 (m), 1097 (w), 1071 (m), 1032 (s), 1010 (m), 950 (vvs), 904 (m), 830 (m), 813 (vs), 784 (vvs), 742 (vvs), 668 (w), 522 (m), 491 (vs), 402 (w), 363 (m), 346 (w), 315 (s), 251 (m), 238 (w) cm^{-1}. *Note.* No elemental analysis was performed, since the crystals lost the 4-methylpyridine solvent of crystallization when removed from the solution.

***cis*-(4-MePyH)$_3$[$Mo_2O_4(\eta^2\text{-}C_2O_4)_2$(4-MePy)$_2$]Br (6). Procedure a:** A glass tube was charged with (PyH)[$MoOBr_4$] (120 mg, 0.235 mmol), $H_2C_2O_4\cdot 2H_2O$ (200 mg, 1.59 mmol), 4-methylpyridine (4 mL), 2-propanol (0.5 mL), and acetonitrile (0.5 mL). The tube was sealed and heated for 90 h in an electric oven maintained at 115 °C. After cooling to room temperature, the reaction mixture consisted of a clear, orange solution. Over a period of two weeks two types of crystals grew from the solution: yellow, needle-like crystals of **5** and orange, block-like crystals of **6**. The total amount of solid material was 62 mg. **Procedure b:** A glass tube was charged with (PyH)[$MoOBr_4$] (120 mg, 0.235 mmol), $H_2C_2O_4\cdot 2H_2O$ (100 mg, 0.794 mmol), and 4-methylpyridine (4 mL). The tube was sealed and heated for 90 h in an electric oven maintained at 115 °C. The reaction mixture was allowed to cool slowly to room temperature. Orange, block-shaped crystals of **6** were separated manually from the colorless, needle-like crystals of 4-methylpyridinium oxalate. Yield: 71% (82 mg). IR: $\tilde{\nu}$ = 2921 cm^{-1} (m), 2846 (m), 1707 (vvs), 1682 (vvs), 1633 (vvs), 1503 (vs), 1417 (vs), 1307 (s), 1277 (vs), 1232 (m), 1202 (m), 1098 (m), 1059 (m), 1032 (s), 1006 (m), 949 (vvs), 932 (vs), 904 (m), 813 (vs), 789 (vs), 748 (vs), 722 (vs), 666 (w), 651 (w), 553 (m), 519 (s), 503 (vs), 483 (vvs), 476 (vvs), 402 (m), 365 (s), 349 (m), 321 (vs), 294 (m), 273 (w), 247 (m), 218 (w) cm^{-1}. $C_{34}H_{38}BrMo_2N_5O_{12}$ (980.5): calcd. C 41.65, H 3.91, N 7.14, found C 41.58, H 3.64, N 6.98.

***trans*-[$(C_6H_5)_4P]_2[Mo_2O_4(\eta^2\text{-}C_2O_4)_2Py_2]\cdot H_2O$ (7):** Compound **1** (250 mg, 0.333 mmol) was dissolved in water (10 mL). After the addition of potassium hydroxide (42 mg, 0.749 mmol), the clear, orange solution turned cloudy. The solution was then filtered and a solution of tetraphenylphosphonium bromide (315 mg, 0.754 mmol) in acetonitrile (7 mL) was added to the filtrate. The volume of the filtrate was reduced to one half by pumping on the vacuum line. The concentrated solution was kept in a closed flask at ambient conditions. Red crystals of **7** grew after two days and were collected by filtration and washed with dichloromethane. Yield: 41% (178 mg). IR: $\tilde{\nu}$ = 3526 cm^{-1} (w), 3396 (w), 1707 (m), 1687 (s), 1672 (vs), 1642 (s), 1603 (m), 1581 (m), 1481 (m), 1436 (s), 1376 (s), 1314 (w), 1249 (m), 1218 (m), 1160 (w), 1107 (vs), 1069 (w), 1042 (w), 1015 (w), 997 (m), 937 (vs), 919 (m), 898 (m), 845 (w), 784 (s), 755 (s), 743 (s), 721 (vs), 691 (vs), 634 (w), 528 (vs), 471 (m), 317 (m), 264 (w). $C_{62}H_{52}Mo_2N_2O_{13}P_2$ (1286.9): calcd. C 57.87, H 4.07, N 2.18, found C 57.68, H 4.28, N 2.09.

***trans*-(PyH)$_2$[$Mo_2O_4(\eta^2\text{-}C_2O_4)_2(H_2O)_2$] (8):** Compound **1** (250 mg, 0.333 mmol) was dissolved in water (10 mL). Methanol (10 mL) and pyridinium sulfate (256 mg, 1.00 mmol) were then added to the clear, orange solution. The solution was left in an open beaker under ambient conditions. Within a few hours orange crystals of **8** started to deposit from the solution. The crystals were collected by filtration and washed with dichloromethane. Yield: 67% (140 mg). IR: $\tilde{\nu}$ = 2900 cm^{-1} (br), 1650 (vvs), 1483 (s), 1418 (s), 1392 (s), 1287 (s), 1258 (s), 1197 (m), 1166 (m), 1058 (m), 1007 (m), 964 (vvs), 945 (vvs), 910 (vs), 856 (m), 788 (vs), 750 (vs), 722 (vs), 678 (vs), 609 (s), 588 (s), 534 (s), 490 (vvs), 447 (m), 393 (m), 350 (w), 311 (s), 260 (s), 180 (w) cm^{-1}. $C_{14}H_{16}Mo_2N_2O_{14}$ (628.2): calcd. C 26.77, H 2.57, N 4.46, found C 26.71, H 2.49, N 4.49.

Isomerization of *cis*-(4-EtPy)$_2$[$Mo_2O_4(\eta^2\text{-}C_2O_4)_2$(4-EtPy)$_2$] (4): Compound **4** (140 mg, 0.162 mmol) was dissolved in water (7.5 mL) and methanol (7.5 mL) and pyridinium sulfate (130 mg, 0.508 mmol) were added to the solution. The solution was allowed to stand in an open beaker under ambient conditions for three

days. Orange crystals of **8** were collected by filtration and washed with dichloromethane. Yield: 81% (82 mg).

$(PyH)_2[Mo_8O_{16}(OCH_3)_8(\mu_8\text{-}C_2O_4)]\cdot 2CH_3OH$ (9): Compound **8** (220 mg, 0.350 mmol) was added to methanol (15 mL) in an Erlenmeyer flask, which was stoppered and the reaction mixture stirred under ambient conditions for three days. The unreacted starting material (150 mg) was filtered off and the resulting filtrate was allowed to stand in an open beaker under ambient conditions overnight. Orange, needle-shaped crystals of **9** grew from the solution. Yield (based on the dried product and taking into the account only the reacted starting material): 84% (37 mg). IR: $\tilde{\nu}$ = 2925 cm^{-1} (s), 2851 (m), 2825 (m), 1661 (vs), 1650 (m), 1610 (w), 1528 (m), 1484 (m), 1444 (m), 1389 (s), 1283 (w), 1253 (w), 1200 (w), 1168 (m), 1027 (vs), 969 (vvs), 814 (vs), 750 (vvs), 721 (vvs), 676 (m), 539 (vvs), 462 (vvs), 380 (m), 339 (m), 275 (s), 221 (m) cm^{-1}. *Note.* No elemental analysis was performed since the crystals quickly lost the methanol solvent of crystallization when removed from the solution.

Computational Details: MO calculations on the *trans* and *cis* isomeric forms of $[Mo_2O_4(\eta^2\text{-}C_2O_4)(4\text{-}MePy)_2]^{2-}$ were performed in order to determine their relative stabilities using three different methods: (i) semi-empirical PM3, (ii) ab initio Hartree–Fock with the 3-21G basis set, and (iii) density functional B3LYP with the 6-31G* basis set and a pseudopotential. The SPARTAN′02 program was used.[34] The atomic coordinates of the anions in **5** and **6** were taken from the X-ray diffraction study. No geometric optimization was applied. The calculated energy differences are too small to have any significance. According to the first method, the energy of the *cis* isomer is 0.95 $kJ\,mol^{-1}$ lower than that of the *trans* isomer. The other two methods show the *trans* isomer as the more energetically favored, by 11.59 $kJ\,mol^{-1}$ using the second method and by 7.24 $kJ\,mol^{-1}$ using the third method.

X-ray Crystallographic Study: Crystals were mounted on the tip of a glass fiber with a small amount of silicon grease and transferred to the goniometer head. Data for **4** and **6** were collected on a Bruker P4 diffractometer equipped with a SMART CCD system.

Table 5. Crystallographic data for compounds **1**–**5**.

	1	**2**	**3**	**4**	**5**
Empirical formula	$C_{24}H_{22}Mo_2N_4O_{12}$	$C_{28}H_{30}Mo_2N_4O_{12}$	$C_{34}H_{44}Mo_2N_4O_{13}$	$C_{32}H_{38}Mo_2N_4O_{12}$	$C_{31}H_{33.5}Mo_2N_{4.5}O_{12}$
Formula mass	750.34	806.44	908.61	862.54	852.99
Crystal system	monoclinic	monoclinic	monoclinic	monoclinic	triclinic
Space group	*C*2/*c*	*C*2/*c*	$P2_1/n$	$P2_1$	$P\bar{1}$
T [K]	200(2)	150(2)	150(2)	94(2)	110(2)
a [Å]	22.0725(2)	22.0750(3)	13.3334(1)	10.3678(8)	12.4664(2)
b [Å]	8.7841(1)	8.4565(1)	16.4482(2)	15.399(1)	17.3974(2)
c [Å]	15.1629(2)	17.3676(3)	17.2333(2)	11.0861(9)	18.0972(3)
α [°]	90	90	90	90	93.8446(6)
β [°]	113.3504(4)	97.7975(8)	92.0718(4)	91.902(2)	108.9105(7)
γ [°]	90	90	90	90	92.8035(6)
V [$Å^3$]	2699.11(5)	3212.16(8)	3776.97(7)	1768.9(2)	3694.4(1)
Z	4	4	4	2	4
μ [mm^{-1}]	1.002	0.848	0.733	0.776	0.742
Collected reflections	5947	6908	16799	22565	28754
Unique reflections, R_{int}	3087, 0.0149	3651, 0.0133	8586, 0.0178	11276, 0.0236	16441, 0.0251
Observed reflections	2699	3354	7264	11088	13525
*R*1 [$I > 2\sigma(I)$]	0.0217	0.0221	0.0284	0.0251	0.0503
*wR*2 (all data)	0.0551	0.0565	0.0739	0.0652	0.1414

Table 6. Crystallographic data for compounds **6**–**9**.

	6	**7**	**8**	**9**
Empirical formula	$C_{34}H_{38}BrMo_2N_5O_{12}$	$C_{62}H_{52}Mo_2N_2O_{13}P_2$	$C_{14}H_{16}Mo_2N_2O_{14}$	$C_{22}H_{44}Mo_8N_2O_{30}$
Formula mass	980.48	1286.88	628.17	1584.11
Crystal system	monoclinic	monoclinic	triclinic	triclinic
Space group	$P2_1/n$	$P2_1/n$	$P\bar{1}$	$P\bar{1}$
T [K]	91(2)	293(2)	293(2)	150(2)
a [Å]	10.0050(5)	14.4105(1)	12.5884(2)	8.6323(1)
b [Å]	14.4475(7)	26.0364(2)	13.0228(2)	12.2594(2)
c [Å]	27.838(1)	15.2125(1)	13.5288(2)	12.2558(2)
α [°]	90	90	89.2790(6)	94.4216(6)
β [°]	96.538(1)	98.4308(4)	70.3024(7)	105.3578(7)
γ [°]	90	90	76.6323(6)	110.2995(7)
V [$Å^3$]	3997.7(3)	5646.01(7)	2026.33(5)	1152.34(3)
Z	4	4	4	1
μ [mm^{-1}]	1.691	0.569	1.316	2.195
Collected reflections	50588	23321	16410	9530
Unique reflections, R_{int}	13204, 0.0224	12915, 0.0218	9171, 0.0176	5250, 0.0138
Observed reflections	11878	10290	6834	4843
*R*1 [$I > 2\sigma(I)$]	0.0273	0.0340	0.0314	0.0268
*wR*2 (all data)	0.0736	0.1006	0.0842	0.0821

Data processing was accomplished with the SAINT program.[35] Absorption corrections were made using SADABS.[36] Data for **1**, **2**, **3**, **5**, **7**, **8**, and **9** were collected on a Nonius Kappa CCD diffractometer. Data reduction and integration were performed with the software package DENZO-SMN.[37] Averaging of the symmetry-equivalent reflections largely compensated for the absorption effects. For all compounds, the coordinates of some or all of the non-hydrogen atoms were found by direct methods using the structure solution program SHELXS.[38] The positions of the remaining non-hydrogen atoms were located by use of a combination of least-squares refinement and difference Fourier maps in the SHELXL-97 program.[38] With the exception of **5** and **9**, all non-hydrogen atoms were refined anisotropically. The asymmetric unit of **5** contains two 4-methylpyridine molecules of crystallization, one of which is badly disordered, in addition to two dinuclear anions and four protonated 4-methylpyridine molecules. The disorder could not be modeled satisfactorily, resulting in relatively large *R* factors and residual density in the final difference Fourier map. The nitrogen and carbon atoms of both solvent molecules were refined isotropically. The oxalate ion in **9** is disordered over two positions. The carbon atoms C(6) and C(7) of the disordered oxalate ion were refined isotropically, each with an occupancy factor of 0.5. The hydrogen atoms were included in the structure factor calculations at idealized positions. Figures depicting the structures were prepared with SHELXTL.[39] Cell parameters and refinement results are summarized in Tables 5 and 6. CCDC-258550 (**1**), -258551 (**2**), -258552 (**3**), -258553 (**4**), -258554 (**5**), -258555 (**6**), -258556 (**7**) -258557 (**8**), and 258558 (**9**) contain the supplementary crystallographic data for this paper. These data can be obtained free of charge from The Cambridge Crystallographic Data Centre via www.ccdc.cam.ac.uk/data_request/cif.

Supporting Information (see also footnote on the first page of this article): Contains Figure S1 {^{1}H NMR spectra of the diluted D_2O/CD_3OD solutions of *trans*-$(MeNC_5H_5)_2[Mo_2O_4(\eta^2\text{-}C_2O_4)_2Py_2]$, recorded at 243 K} and Figure S2 {^{1}H NMR spectra of D_2O/CD_3OD solutions of *trans*-$(MeNC_5H_5)_2[Mo_2O_4(\eta^2\text{-}C_2O_4)_2Py_2]$ titrated with pyridine, recorded at 243 K}.

Acknowledgments

The work was supported by the Slovenian Ministry of Education, Science and Sport (grant P1-0134) and by the National Science Foundation (Grant CHE-0242153). We are grateful to Prof. Alojz Demšar for his help with the simulation of NMR spectra.

[1] E. I. Stiefel, *Prog. Inorg. Chem.* **1977**, *22*, 1–223.
[2] H. K. Chae, W. G. Klemperer, T. A. Marquart, *Coord. Chem. Rev.* **1993**, *128*, 209–224.
[3] B. Modec, J. V. Brenčič, *J. Cluster Sci.* **2002**, *13*, 279–302 and references cited therein.
[4] D. J. Darensbourg, R. L. Gray, T. Delord, *Inorg. Chem. Acta* **1985**, *98*, L39–L42.
[5] B. Modec, J. V. Brenčič, L. Golič, *Polyhedron* **2000**, *19*, 1219–1225.
[6] B. Modec, J. V. Brenčič, R. C. Finn, R. S. Rarig, J. Zubieta, *Inorg. Chim. Acta* **2001**, *322*, 113–119.
[7] B. Modec, J. V. Brenčič, D. Dolenc, J. Zubieta, *J. Chem. Soc., Dalton Trans.* **2002**, 4582–4586.
[8] M.-Y. Lee, S.-L. Wang, *Chem. Mater.* **1999**, *11*, 3588–3594.
[9] L. A. Mundi, R. C. Haushalter, *Inorg. Chem.* **1990**, *29*, 2879–2881.
[10] a) L. A. Mundi, R. C. Haushalter, *J. Am. Chem. Soc.* **1991**, *113*, 6340–6341; b) E. W. Corcoran Jr., *Inorg. Chem.* **1990**, *29*, 157–158; c) R. C. Haushalter, K. G. Strohmaier, F. W. Lai, *Science* **1989**, *246*, 1289–1291.
[11] B. Modec, J. V. Brenčič, J. Koller, *Eur. J. Inorg. Chem.* **2004**, 1611–1620.
[12] L. Lisnard, P. Mialane, A. Dolbecq, J. Marrot, F. Secheresse, *Inorg. Chem. Commun.* **2003**, *6*, 503–505.
[13] F. A. Cotton, S. M. Morehouse, *Inorg. Chem.* **1965**, *4*, 1377–1381.
[14] B. Kamenar, B. Kaitner, N. Strukan, *Croat. Chem. Acta* **1991**, *64*, 329–341.
[15] W. S. McDonald, *Acta Crystallogr., Sect. B* **1978**, *34*, 2850–2853.
[16] R. Yang, X. Yu, *Chin. J. Struct. Chem.* **1985**, *4*, 1–4.
[17] A. Dolbecq, B. Salignac, E. Cadot, F. Secheresse, *Bull. Pol. Acad. Sci.* **1998**, *46*, 237–271.
[18] Q. Chen, S. Liu, J. Zubieta, *Angew. Chem. Int. Ed. Engl.* **1988**, *27*, 1724–1725.
[19] X.-P. Zhan, C.-Z. Lu, W.-B. Yang, H.-W. Ma, C.-D. Wu, Q.-Z. Zhang, *Dalton Trans.* **2003**, 1457–1458.
[20] K. Mennemann, R. Mattes, *J. Chem. Res.* **1979**, *100*, 1343.
[21] T. Shibahara, S. Ooi, H. Kuroya, *Bull. Chem. Soc. Jpn.* **1982**, *55*, 3742–3746.
[22] C. du Peloux, A. Dolbecq, E. Cadot, J. Marrot, F. Secheresse, *J. Mol. Struct.* **2003**, *656*, 37–44.
[23] We observed that pyridine *N*-methylation with methanol took place in the presence of oxalic acid at elevated temperature. The fact that *N*-methylpyridinium salts result from a nucleophilic attack of pyridine on methyl halide formed from methanol and hydrogen halide does not provide a valid explanation. The latter reaction requires strongly acidic conditions, while the reaction medium in our case contains mostly pyridine. Moreover, the halogenation of alcohols is known to proceed more readily with tertiary and secondary alcohols, but not with methanol. The exact nature of this process is currently under investigation.
[24] A downfield shift was observed for the signals of free pyridine [243 K spectrum: δ = 7.67 (C-3), 8.14 (C-4), 8.62 (C-2) ppm], suggesting that pyridine is not entirely free. The corresponding pyridine frequencies in water solution appear at δ = 7.24, 7.66, and 8.32 ppm.
[25] The integral of signal C2, which belongs to free pyridine, is smaller than the integrals of signals A2 and B2. This observation rules out an alternative explanation: an equilibrium between only one isomeric form of $[Mo_2O_4(\eta^2\text{-}C_2O_4)_2Py_2]^{2-}$ (set A), the mono-substituted complex (set B), and the bis(aqua)-ligated complex. In the latter situation the integral of C2 would be larger than the integral of B2 because the amount of free pyridine is twice the amount of the bis(aqua)-ligated complex plus the amount of the mono-substituted complex.
[26] For comparison, the carbonate carbon resonances in water solution of $[(Mo_2O_4)_3(\mu_6\text{-}CO_3)(\mu_2\text{-}CO_3)_3(\mu_2\text{-}OH)_3]^{5-}$ with two distinctly different carbonato ligands appear in the same spectral region: two major signals at δ = 160 and 165 ppm with a 1:3 intensity ratio and three minor ones at δ = 160.5, 164.5, and 165.5 ppm. [M. J. Manos, A. D. Keramidas, J. D. Woollins, A. M. Z. Slawin, T. A. Kabanos, *J. Chem. Soc., Dalton Trans.* **2001**, 3419–3420.] The ^{13}C NMR spectrum of an aqueous solution of ammonium oxalate reveals a resonance at δ = 173.9 ppm.
[27] P. H. M. Budzelaar, *gNMR* Version 5.0.1.0. NMR Simulation Program, IvorySoft, Oxford, **2002**.
[28] a) R. G. James, W. Wardlaw, *J. Chem. Soc.* **1927**, 2145–2156; b) H. M. Spittle, W. Wardlaw, *J. Chem. Soc.* **1928**, 2742.
[29] P. C. H. Mitchell, *J. Chem. Soc. A* **1969**, 146–152.
[30] a) N. F. Curtis, *J. Chem. Soc. A* **1968**, 1584–1587; b) P. Roman, A. Luque, C. Guzman-Miralles, J. I. Beitia, *Polyhedron* **1995**, *14*, 2863–2869.
[31] K. Nakamoto, *Infrared and Raman Spectra of Inorganic and Coordination Compounds. Part B: Applications* in *Coordination, Organometallic and Bioinorganic Chemistry*, 5th ed., Wiley In-

terscience, New York, Chichester, Weinheim, Brisbane, Singapore, Toronto, **1997**, pp. 53–57.
[32] B. Modec, J. V. Brenčič, *Eur. J. Inorg. Chem.* **2005**, 1698–1709.
[33] G. R. Hanson, A. A. Brunette, A. C. McDonell, K. S. Murray, A. G. Wedd, *J. Am. Chem. Soc.* **1981**, *103*, 1953–1959.
[34] *Spartan'02*, Wavefunction, Inc., Irvine, CA, **2002**.
[35] *SMART* and *SAINT*, Siemens Analytical Instruments Inc., Madison, WI, **1990**.
[36] G. M. Sheldrick, *SADABS, A Program for Absorption Correction with the Siemens SMART Area-Detector system*, Universität Göttingen, **1996**.
[37] Z. Otwinowski, W. Minor, *Methods Enzymol.* **1997**, *276*, 307–326.
[38] G. M. Sheldrick, *SHELXS-97* and *SHELXL-97*, Universität Göttingen, **1997**.
[39] *SHELXTL, Software Package for Crystal Structure Determination*, Version 5.03, Siemens Analytical X-ray Instrument Division, Madison, WI, **1994**.

Received: January 10, 2005
Published Online: July 12, 2005

